Supporting Information

Metabolic activation of elemicin leads to the inhibition of stearoyl-CoA desaturase 1

Xiao-Nan Yang[a,e], Yi-Kun Wang[a,b], Xu Zhu[a,b], Xue-Rong Xiao[a], Man-Yun Dai[a,b], Ting Zhang[a,b], Yan Qu[a], Xiu-Wei Yang[c], Hong-Bo Qin[a], Frank J. Gonzalez[d], Fei Li[a,*]

[a]State Key Laboratory of Phytochemistry and Plant Resources in West China, Kunming Institute of Botany, Chinese Academy of Sciences, Kunming 650201, China
[b]University of Chinese Academy of Sciences, Beijing 100049, China
[c]School of Pharmaceutical Sciences, Peking University Health Science Center, Peking University, Beijing 100191, China
[d]Laboratory of Metabolism, Center for Cancer Research, National Cancer Institute, National Institutes of Health, Bethesda, MD 20892, USA
[e]Guangxi Key Laboratory of Medicinal Resources Protection and Genetic Improvement, Guangxi Botanical Garden of Medicinal Plant, Nanning 530023, China

*Address correspondence to:
Fei Li, Ph.D., Kunming Institute of Botany, Chinese Academy of Sciences, Kunming 650201, China. Tel: +86-871-65216953, Email: lifeib@mail.kib.ac.cn.

Synthesis of 1′-hydroxyelemicin

1′-Hydroxyelemicin was synthesized by substrate 3,4,5-trimethoxybenzaldenyde. The reaction was carried out as fallows. 3,4,5-Trimethoxybenzaldenyde (0.56 mmol, 110 mg dissolved in anhydrous tetrahydrofuran 2 mL) under nitrogen (N_2) was supplemented vinylmagnesium bromide (0.56 mL, 1 mol·L^{-1},) dropwise at 0℃. After being stirred for 1 h at 25℃, the mixture was terminated with saturated aqueous NH_4Cl and extracted with ethyl acetate. The combined organic layer was washed sequentially with saturated aqueous sodium carbonate solution, water, and brine, and dried over Na_2SO_4, and the crude product filtered and concentrated. Further separation was accomplished by silica gel column chromatography using mobile phase EtOAc: Petroleum ether 1=10, at last afford the total pure product (103 mg) as a colorless oil liquid. The yield of 1′-hydroxyelemicin was 82% from raw material. The synthesized compounds were characterized by ^{1}H-NMR, ^{13}C-NMR and HR-ESI-MS. The purity of 1′-hydroxyelemicin was > 98% measured by ultra-performance liquid chromatography (UPLC). ^{1}H-NMR ($CDCl_3$, 600 MHz): δ 3.86 (3H, s, OCH_3), 3.82(6H, s, $2OCH_3$), 6.60 (2H, s, 2H/4H), 5.12 (1H, d, H1′) , 6.03 (1H, d, H2′), 5.36/5.20 (2H, d, H3′).^{13}C-NMR ($CDCl_3$, 150MHz): δ 138.33(C-1), 103.13 (C-2), 153.32 (C-3), 137.2 (C-4), 153.32 (C-5), 103.13 (C-2/C-6), 75.39 (C-1′), 140.01 (C-2′), 115.24 (C-3′), 56.07 (3-OCH_3), 60.81 (4-OCH_3), 56.07 (5-OCH_3). HR-ESI-MS: *m/z* 225.1116 $[M+H]^+$ (calculated for $C_{12}H_{17}O_4$, *m/z* 225.1121).

Figure legends

Fig. S1. Plasma aminotransferase (ALT) activity after elemicin (E, 500 mg/kg) and 1′-hydroxyelemicin (E′, 100 mg/kg).

Fig. S2. Comparison between elemicin (E) and 1′-hydroxyelemicin (E′) toxicity at the oral dose of 100 mg/kg for three days.

Fig. S3. Reactive metabolite-GSH adduct *in vivo* and *in vitro*.

Fig. S4. MS/MS spectra and fragmentation patterns of typical LPCs.

Fig. S5. mRNA expression from genes related to LPC synthesis and metabolism.

Fig. S6. Influence of oleic acid supplementation on liver size and hepatic TG content.

Fig. S7. Plots of 1′-hydroxyelemicin formation from different elemicin concentrations.

Fig. S8. Molecular docking of elemicin with CYPs active cavity.

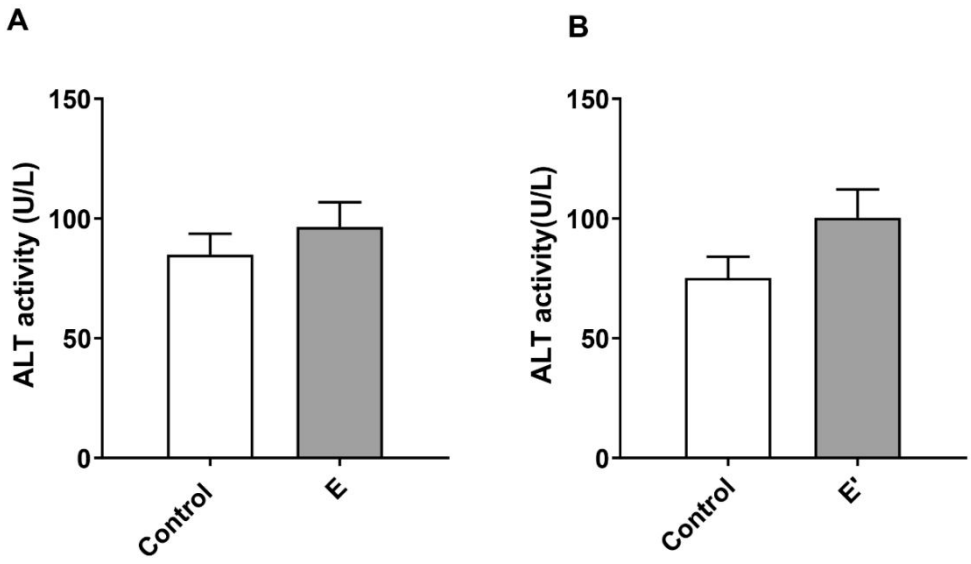

Fig. S1. Plasma aminotransferase (ALT) activity after elemicin (E, 500 mg/kg) and 1′-hydroxyelemicin (E′, 100 mg/kg). (A) $p > 0.05$, no significant difference, compared with vehicle control. (B) $p > 0.05$, no significant difference, compared with vehicle control.

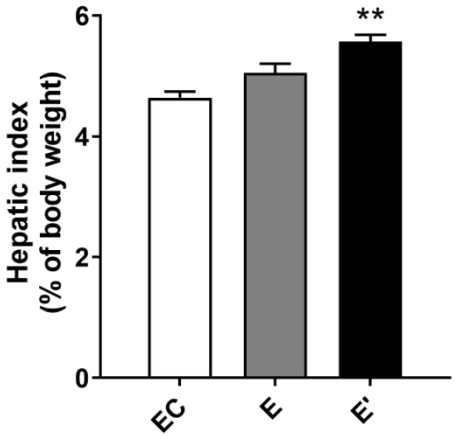

Fig. S2. Comparison between elemicin (E) and 1′-hydroxyelemicin (E′) toxicity at the dose of 100 mg/kg for three days. **$p < 0.01$, significant difference, compared with vehicle control.

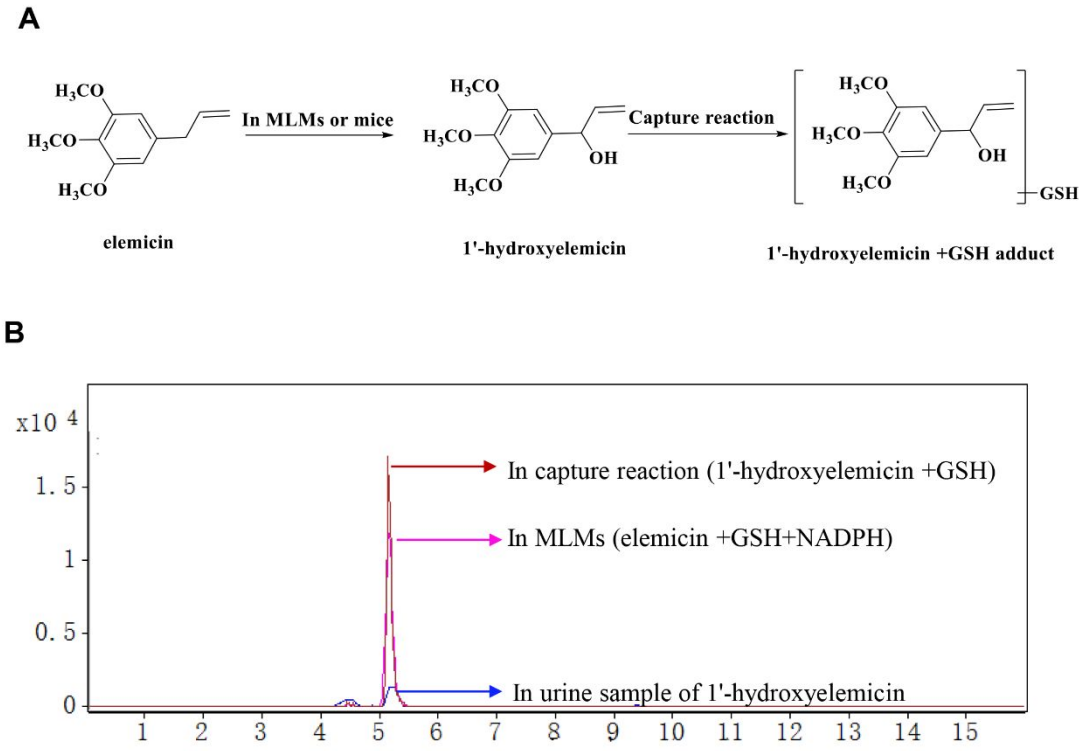

Fig. S3. Reactive metabolite-GSH adduct *in vivo* and *in vitro.* (A) The proposed scheme of 1′-hydroxyelemicin -GSH adduct. (B) Extraction ion chromatography of 1′-hydroxyelemicin -GSH adduct in MLMs, capture reaction, urine sample.

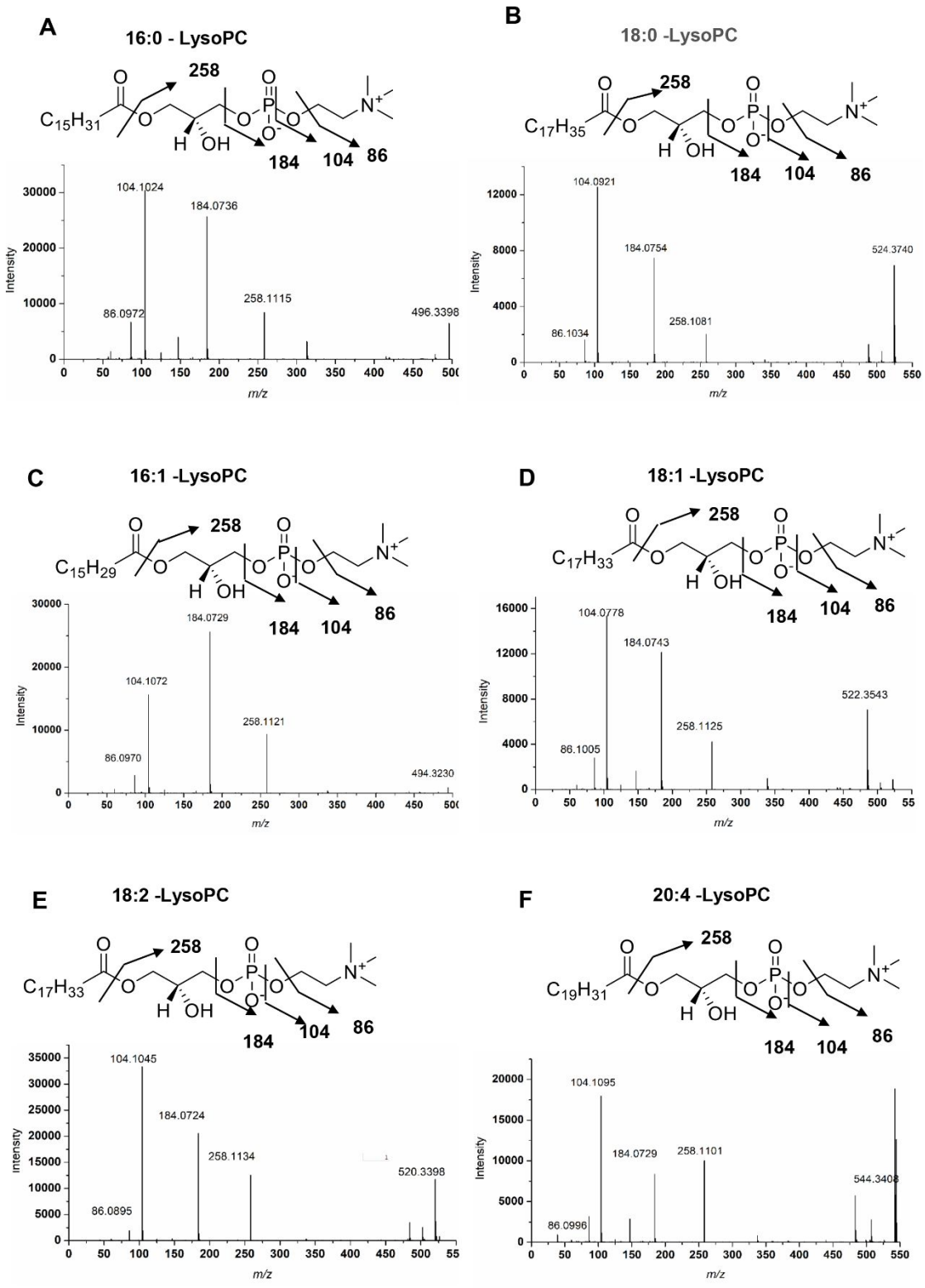

Fig. S4. MS/MS spectra and fragmentation patterns of typical LPCs. (A) 16:0-LysoPC. (B) 18:0-LysoPC. (C) 16:1-LysoPC. (D) 18:1-LysoPC. (E) 18:2-LysoPC. (F) 20:4-LysoPC.

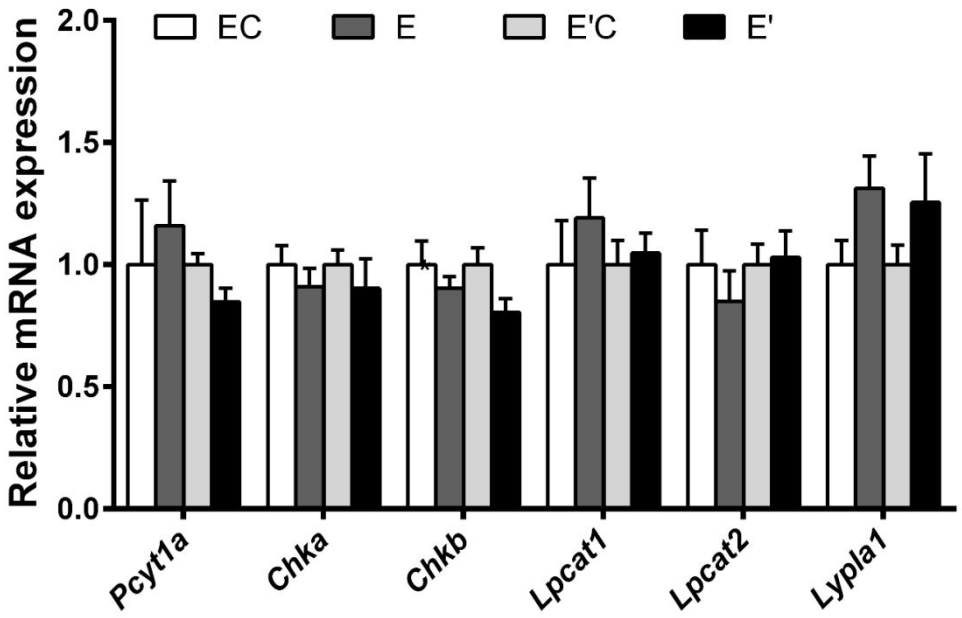

Fig. S5. mRNA expression from genes related to LPCs synthesis and metabolism. $p > 0.05$, no significant difference, elemicin treatment (E) versus its vehicle control, 1′-hydroxyelemicin treatment (E′) versus its vehicle control.

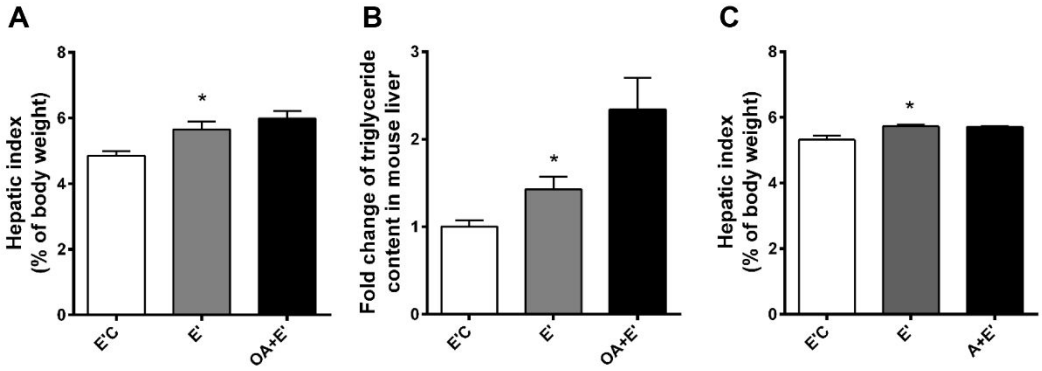

Fig. S6. Influence of oleic acid supplementation in mice. Liver size (A) and hepatic TG content (B). Influence of A939572 on the liver size (C). *$p < 0.05$, significant difference, 1′-hydroxyelemicin treatment (E′) compared with vehicle control (E′C).

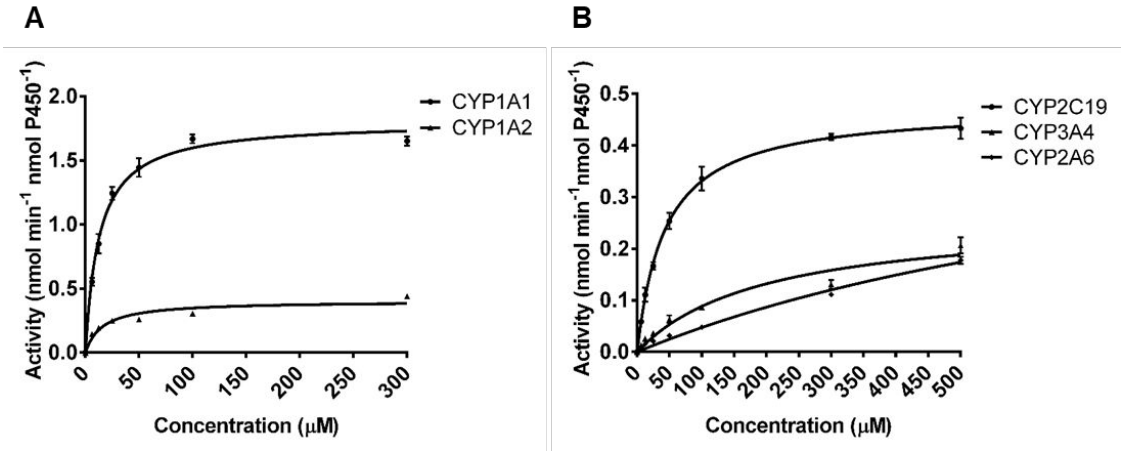

Fig. S7. Plots of 1′-hydroxyelemicin formation from different elemicin concentrations. (A) CYP1A1 (●) and CYP1A2 (▲). (B) CYP2C19 (●), CYP3A4 (▲), and CYP2A6 (♦).

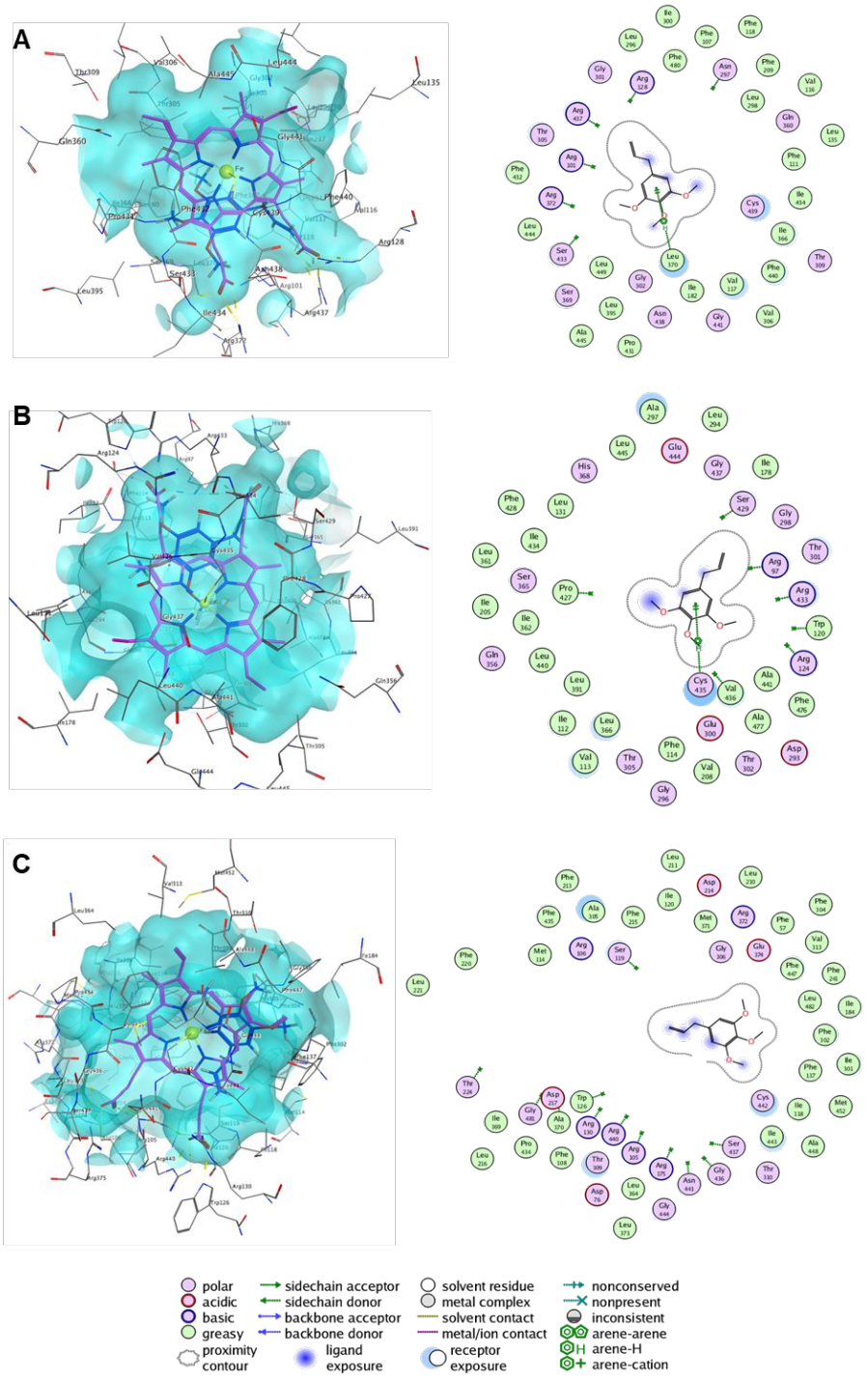

Fig. S8. Molecular docking of elemicin with CYPs active cavity. (A) CYP2A6 pocket and elemicin. (B) CYP2C19 pocket and elemicin. (C) CYP3A4 pocket and elemicin. Elemicin was presented as blue structure, and endogenous ligand ferroheme of CYPs was presented as red structure.

Table S1. Sequences of the qPCR primers.

Gene	Pubmed ID	Forward (5′ to 3′)	Reverse (5′ to 3′)
18S	19791	ATTGGAGCTGGAATTACCGC	CGGCTACCACATCCAAGGAA
Chka	12660	AAAGTGCTCTTGCGGCTCTA	GACCTCTCTGCAAGAATGGC
Chkb	12651	GCAGAGGTTCAGAAGGGTGA	CCCCAGAAAAAGTGAGATGC
Lypla1	18777	CCTTCACGGATTGGGAGATA	GGGGCATGTGGACAGATGTA
Lpcat1	210992	CACGAGCTGCGACTGAGC	ATGAAAGCAGCGAACAGGAG
Lpcat2	270084	ACCTGTTTCCGATGTCCTGA	CCAGGCCGATCACATACTCT
Pcyt1a	13026	AGCCCTATGTCAGGGTGACT	GGCATGACCAGAGTGAAACA
Scd1	20249	GCTCTACACCTGCCTCTTCG	CAGCCGAGCCTTGTAAGTTC

Table S2. Identities of LPCs in mouse plasma.

No.	Observed *m/z*	Rt (min)	Formula	Mass error (ppm)	Identity
1	496.3398	10.79	$C_{24}H_{50}NO_7P[H]^+$	0.11	16:0-LPC
2	524.3710	12.13	$C_{26}H_{54}NO_7P[H]^+$	-0.09	18:0-LPC
3	494.3248	9.92	$C_{24}H_{48}NO_7P[H]^+$	1.46	16:1-LPC
4	522.3558	11.13	$C_{26}H_{52}NO_7P[H]^+$	0.77	18:1-LPC
5	520.3392	10.33	$C_{26}H_{50}NO_7P[H]^+$	-1.05	18:2-LPC
6	544.3395	10.36	$C_{28}H_{50}NO_7P[H]^+$	-0.45	20:4-LPC

Table S3. The number of hydrogen bond donor and receptors in the model of molecular docking.

Receptor	Covalent bonds	Ligand exposure points
CYP1A1	2	7
CYP1A2	1	4
CYP2A6	1	4
CYP2C19	1	3
CYP3A4	0	5